Comparison of OpenFOAM and ANSYS Fluent

Prasanna Welahettige, Knut Vaagsaether

Department of Process, Energy and Environmental Technology
University College of Southeast Norway
Porsgrunn, Norway
prasanna.welahetti@gmail.com

Abstract

Gas-gas single phase mixing were numerically evaluated with static mixer and without static mixer using OpenFOAM and ANSYS Fluent codes. The main goal was the gas-gas mixing simulation comparison between ANSYS Fluent and OpenFOAM. The same ANSYS mesh was used for each case in both codes. The "reactingFoam" solver and species transport models were used for handling the species in OpenFOAM and ANSYS Fluent respectively. The reactingFoam solver is a transient solver and ANSYS Fluent was simulated at steady state condition. Standard k-ε model was used to predict the turbulence effect in both computational fluid dynamics codes. OpenFOAM gave a higher mixing level compared to ANSYS Fluent. Chemical species momentum predictions are more diffusion in OpenFOAM and more convective in ANSYS Fluent.

Keywords: OpenFOAM, ANSYS Fluent, CFD, mass fraction, standard deviation, mixing

1 Introduction

OpenFOAM (OF) is a free computational fluid dynamics (CFD) code developed by OpenCFD Ltd and OpenFOAM Foundation. This CFD code is getting well known in academic and industrial sector due to a broad range of fluid dynamics applications, open source, no limitation for parallel computing, and no limitation of number of species in the chemistry models (Lysenko et al., 2013). ANSYS Fluent (AF) is a commercial code and it is developed for the CFD simulation with powerful graphical user interface. It was developed and maintained by ANSYS Inc. It is possible to achieve the same result from both OF and AF by examining "the exterior flow field around simplified passenger sedan" geometry (Ambrosino and Funel, 2006). Reynolds-averaged Navier-Stokes equations (RANS equations) with the k-ε model can be used for both OF and AF CFD codes. OF predicts more accurate results for the velocity and AF predicts more accurate results for the turbulent kinetic energy (Balogh et al., 2012). According to the analyze of "turbulence separated flows" using OF and AF, turbulence models give closely equal results from the both CFD codes (Lysenko et al., 2013). The main objective of this work is to compare the OF simulation ability with the AF simulation for gas-gas single phase mixing. OpenFOAM 2.4.0 and ANSYS Fluent R16.2 academic version were used for the simulations. These geometry designs are unique models for an industrial application and there are no published experimental results.

2 Solvers selection

The solver selection is an important step in this study. Chemical and physical properties of the system are considered for the solver selection. The continuity equation is required to keep the mass balance constantly. The momentum equation contributes to calculate the velocities and the pressures. This system was operated at an isothermal condition. However, the energy equation was required to predict the densities at the operating pressure and temperature. A multispecies model was required because of air-ammonia mixing. The flow was turbulent. Therefore, a turbulence model was required to predict the turbulence properties. The fluid flow highly interacts with walls and mixer plates. Therefore, a wall treatment method is required.

2.1 The species transport model

A species transport equation is given in Equation-1. It describes the convection and the diffusion of the species i for a unsteady condition without a reaction (Fluent, 2006; Versteeg and Malalasekera, 2007).

$$\frac{\partial \rho Y_i}{\partial t} + \mathrm{div}(\rho U Y_i) = -\mathrm{div}(J_i) + S_i \quad (1)$$

Here, ρ is the density of species i, Y_i is the mass fraction of species i, U is the three dimensional velocity components, t is time, J_i is the diffusion flux of species i, and S_i is the source term of species i. The mass diffusion in a turbulent flow is given as,

$$J_i = -\rho D_i \mathrm{grad}(Y_i) - \frac{\mu_t}{Sc_t}\mathrm{grad}(Y_i) \quad (2)$$

Here μ_t is the turbulent viscosity and Sc_t is the turbulent Schimidt number. The reaction term was neglected because of only the air-ammonia mixing.

2.2 Solvers parameters comparison

A comparison of solvers parameters is shown in Table 1. OF was a transient simulation and AF simulation was a steady state simulation. Most of the OF chemical solvers are transient solvers. However, AF has both transient and steady state solvers for the chemical species. A steady state solver was selected for AF to save the computational time. Ammonia and air are in the AF chemical species database. However, OF does not have a database for chemical species. Therefore, molecular weight, heat capacity, heat of fusion, dynamic

viscosity and Prandtl number were added as the species properties.

"reactingFoam" is a compressibility based solver. Compressibility is defined as inverse of the multiplication of the temperature and the universal gas constant $(RT)^{-1}$ (Greenshields, 2015). The temperature was a constant and the fluid mixer gases were considered as perfect gases in this study. Therefore, the compressibility was constant for the "reactingFoam" simulations. The pressure velocity coupling was handled in two different ways in both CFD codes. PIMPLE algorithm was created by merging the Pressure Implicit with Splitting of Operators (PISO) algorithm and the Semi Implicit Method for Pressure Linked Equations (SIMPLE) algorithm (Versteeg and Malalasekera, 2007). The PIMPLE algorithm operates at PISO mode if the non-orthogonal correction number higher than one (Greenshields, 2015). In this simulation, the non-orthogonal correction number was equal to two. Therefore the pressure velocity coupling was handled by the PISO algorithm in OF. The PISO contains an extra correction step compare to the SIMPLE. Therefore, OF calculations were with an extra correcting than AF calculations in these simulations. These algorithms should not influence the solutions. It influences to the solution calculation methods.

Table 1. Simulation settings comparison between OF and AF.

	OF	AF
Solver type	Compressibility based Transient	Pressure based Steady state
Models	Energy equation Viscous – standard k-ε reactingFoam (solver)	Energy equation Viscous – standard k-ε Species transport
Materials	NH_3, Air	NH_3, Air
Solution Method	PIMPLE limitedLinear	SIMPLE Second order upwind
Solution control	Selected time step	Default under relaxation factors

3 Methods

The basic sketch is shown in Figure 1 to demonstrate the flow directions. In this sketch, the ammonia-injecting pipe and the static mixer modules are not presented.

3.1 Geometries drawing

The ANSYS DesignModeler (DM) tool was used to make the drawings. The purpose of the designs was to mix air and ammonia in the horizontal circular tube. The geometries were drawn based on the data given by YARA International ASA. The parts of the geometry are ammonia injecting pipe, static mixer plates and cylindrical tube walls.

The geometries were drawn in three cases as "without ammonia injecting pipe and without static mixture modules" (case-1), "with ammonia injecting pipe and without static mixer modules" (case-2) and "with ammonia injecting pipe and with static mixer modules" (case-3).

The total length of the large pipe is 5.5 m and diameter is 0.996 m. The length of the ammonia-injecting pipe is 1.473 m and diameter is 0.25 m (the small cylindrical pipe with holes). Figure 2 shows the geometries for above-mentioned three cases. There are a 10 numbers of holes in the ammonia-injecting pipe and the diameter of a hole was 80 mm. The mixer plates were drawn as zero thickness walls to reduce the number of elements in the meshes. There were four number of mixer modules and the mixer plates arrangements were similar in each module but module 2 and 4 were rotated around the pipe central axis by 90°.

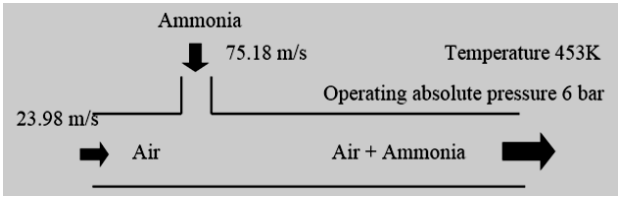

Figure 1. Air and ammonia inlets, outlet and flow directions.

3.2 Mesh generation

The same mesh was used for simulation in both CFD codes in each case for an accurate comparison. Three meshes were generated with respect to the above mentioned three geometry cases. These meshes are shown in Figure 3 and the element types are shown in Table 2. The minimum and maximum element sizes are 2.88 mm and 288 mm respectively for all 3 cases. More tetrahedral elements are added when the complexity is increased in the geometries. Inflation layers are added to better prediction in near the walls and the mixer plates. The total number of cells is increased by five times due to inclusion of the static mixer.

3.3 Boundary conditions and initial values for OF and AF

The boundary conditions were named as "velocity_inlet_air", "velocity_inlet_nh3", "pressure_outlet" and "walls". The velocity inlet type was selected by assuming an incompressible fluid. A comparison of boundary conditions is shown Table 3. The air inlet velocity was 23.98 m/s. The turbulence intensities were 1.7 % and 1.9 % in air inlet and ammonia inlet respectively. All the outer cylinder surfaces and mixer plates were considered as the walls. The walls were assumed as "no slip" condition and there was no heat transfer through the walls.

3.4 Mixing Evaluation Method

Mixing evaluation can be done using a "mixer parameter" (Kok and van der Wal, 1996). It is based on the standard deviation of species mass fraction. The sample points are considered in a line. This model was

considered as the basic model for the mixing evaluation in this study. The same basic mixing evaluation method was applied for this study in a different manner to evaluate the mixing of ammonia and air. Ten number of mixing evaluation planes were defined after the static mixer modules. The mixing evaluation planes were circular cross sections of the large cylindrical pipe as shown in Figure 4. The gap between two subsequent planes is 100 mm. These mixing evaluation planes are located after the static mixer modules to evaluate the fluid coming out from static mixer modules. Standard deviation values of ammonia mass fraction were calculated for the each mixing evaluation planes. All cells available in a mixing evaluation plane were considered to calculate a standard deviation value. Ten number of standard deviation values were calculated for a geometry model. Standard deviation values were plotted against x/D values for the each geometry models.

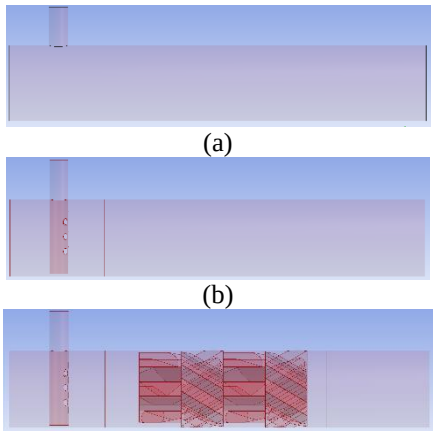

(a) (b) (c)

Figure 2. Geometry; (a) Case-1, (b) Case-2, (c) Case-3.

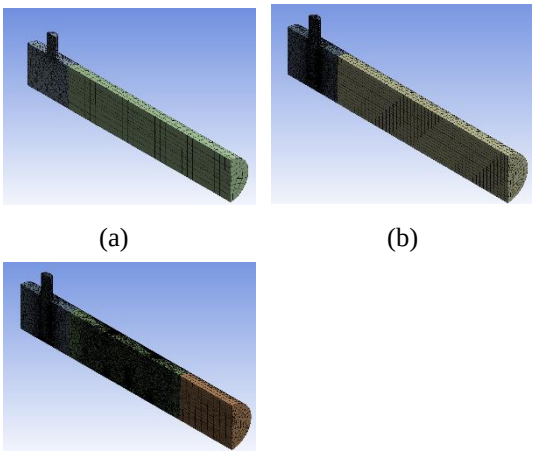

(a) (b) (c)

Figure 3. Mesh cross sectional view; (a) Case-1, (b) Case-2, (c) Case-3.

Here, x is the axial position from air inlet and D is the large circular pipe diameter. If the curve gives a lower values line, the design gives a better mixing than the others. If the curve gives a higher values line, the design gives a lower mixing than the others. The mixing evaluation model proposed in this study was more accurate than the basic model and easy to compare with the similar geometry models.

Table 2. Elements details of meshes.

Type of cells	Case-1	Case-2	Case-3
Hexahedra	1410	10192	4505
Prisms	60	98	136
Pyramids	47	208	265
Tetrahedral	8321	235100	1214040
Total cells	9838	245598	1218946

This method gives an overall idea about the mixing. All the cells available in each mixing evaluation planes contribute for the calculations. This method is more accurate if the gap between two planes is reduced and the numbers of evaluation planes are increased.

Table 3. Boundaries comparison between OF and AF.

Boundary		**OF**	**AF**
Name	***Variable***		
Velocity_inlet_nh3	Velocity	fixedValue - 75.18 m/s	75.18 m/s
	Pressure	zeroGradient	Gauge Pressure–0
	NH_3	fixedValue – 1	1
Pressure_outlet	Velocity	PressureInletOutletVelocity, $internalField	-
	Pressure	TotalPressure	Gauge Pressure–0

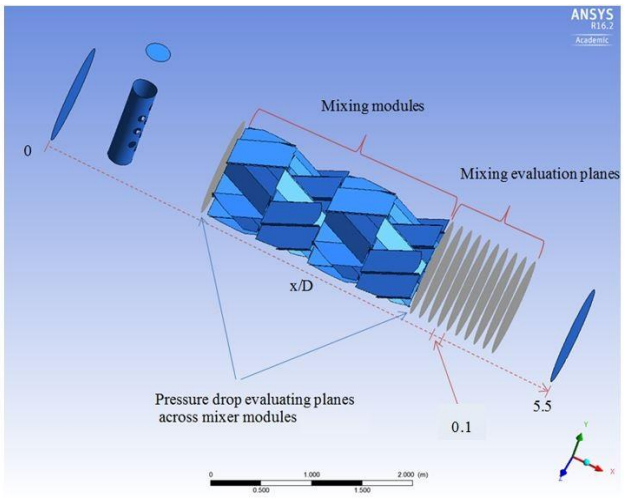

Figure 4. Mixing evaluation planes.

4 Results

Observations of the mixing behavior were the main objective in results analysis. Computational time optimization was not focused in this study.

4.1 Case-1

Ammonia mass fraction contours are shown in Figure 5 for both CFD codes. The OF simulation showed a bit more diffusive flow patterns compared to the AF. The AF simulation showed longer convective ammonia channels. These channels became less diffusive toward the outlet in AF compared to OF. A higher mixing level was shown in the OF simulation compared to AF as shown in Figure 6 (OF showed lower standard deviation values). It was due to a higher diffusive behavior of OF simulation. Mixing level was further increased towards the outlet because the residence time increased. This was basically due to macro mixing. When the residence time increases, the interaction between molecules further increases.

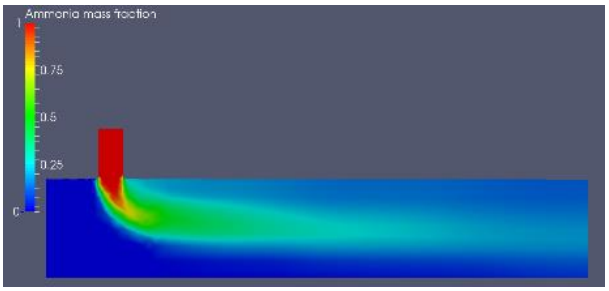

(a)

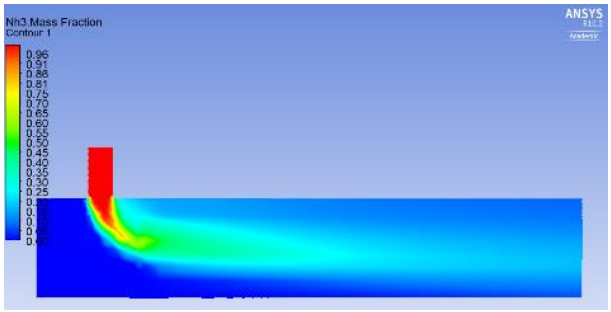

(b)

Figure 5. Ammonia mass fraction contours case -1; (a) OF, (b) AF.

4.2 Case-2

Theoretically, a perfect mixing gives a stoichiometric mixture. The stoichiometric ammonia mass fraction was equal to 0.16 for these simulations. Ammonia mass fraction was plotted along the central axis line in large circular pipe as shown in Figure 7.

Ammonia mass fraction was zero in $-0.65 < x/D < 0$ range, because of large upstream airflow. This implies that there was no backflow of ammonia. At the ammonia inlet tube $-0.125 < x/D < 0.125$, ammonia mass fraction was equal to one. This means that there was no initial air remaining in the ammonia-injecting pipe at the steady state. There was an increment in ammonia mass fraction close to x/D = 0.35. This was due to the position of monitoring line, which was placed between two conservative holes of the injector. At x/D > 2.5, ammonia mass fraction was a constant value in the AF simulation. However, there was a fluctuation in the OF simulation. This was basically due to "wiggles" formation in OF simulation. These "wiggles" patterns generated with transient simulation in OF. As well as, the "wiggles" helped to increase the mixing in OF compared to AF. However, the OF result was fluctuating around the AF results. Therefore the average ammonia mass fraction value of OF was almost similar to the AF result.

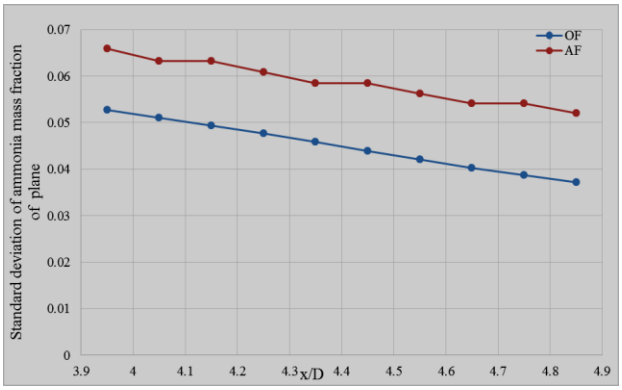

Figure 6. Mixing evaluation – case-1 (standard deviation of ammonia mass fraction).

4.3 Case-3

Ammonia mass fraction contours are shown in Figure 8. Both CFD codes show similar contours in this case. Standard deviation of ammonia mass fraction is shown in Figure 9. Case-3 showed lowest standard deviation values from both CFD codes compared to the previous cases (case-1 and case-2). This implies that the static mixer has improved the mixing. OF simulation result showed higher mixing (lower standard deviation values) in case-3 compare to AF.

Ammonia mass fraction contours at x/D = 4.85 (this location is the 10th mixing evaluation plane in Figure 4) is shown in Figure 10. The range of ammonia mass fraction was shown from 0.1 to 0.2 to compare with perfect mixing. A perfect mixing was given at ammonia mass fraction equal to 0.16 from a stoichiometric mixture. Higher perfect mixing regions were shown in OF compared to AF. Further, ammonia mass fraction (0 to 1 range) was plotted along the vertical line (the vertical line is shown in Figure 10) at x/D = 4.85 as shown in Figure 11. Here y is the vertical axis position (y negative means bellow the center of the circular plane). It also showed that OF simulation showed higher ammonia mass fraction regions than AF.

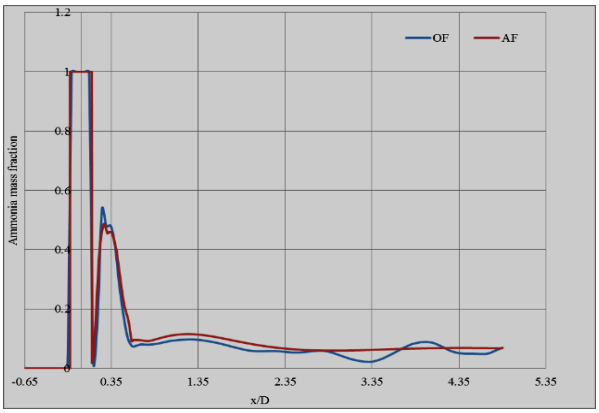

Figure 7. Ammonia mass fraction along the central axis – case-2.

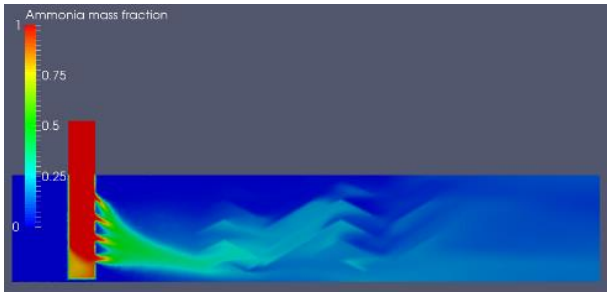

(a)

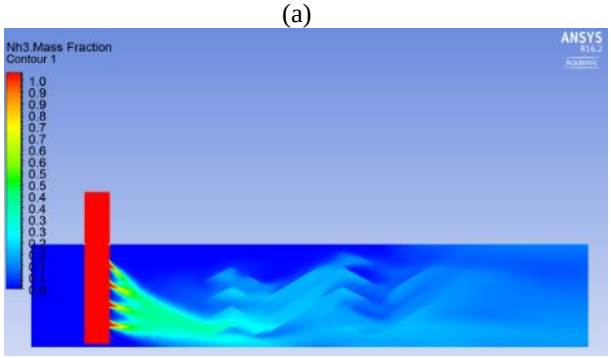

(b)

Figure 8. Ammonia mass fraction case-3; (a) OF, (b) AF.

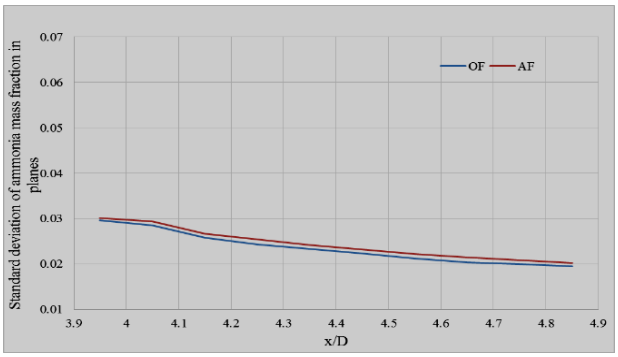

Figure 9. Mixing evaluation - case 3 (standard deviation of ammonia mass fraction).

The average turbulent kinetic energy of the mixing evaluation planes (the mixing evaluation planes are shown in Figure 4) are shown in Figure 12. Higher average turbulent kinetic energy was predicted by OF than AF. Turbulent kinetic energy is reduced toward the outlet due to decay of turbulence.

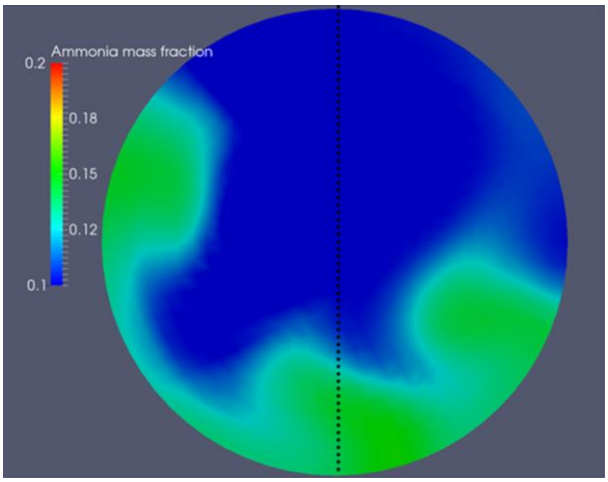

(a)

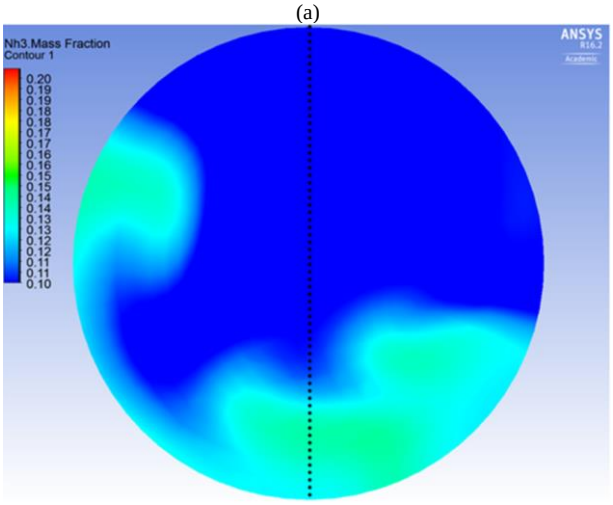

(b)

Figure 10. Ammonia mass fraction contours at x/D = 4.85; (a) OF, (b) AF.

5 Discussion

5.1 Mesh quality requirement comparison between OF and AF

Quality of the mesh is one of the key parameter to control the accuracy and the stability of the computational schemes (Fluent, 2006). Skewness is used to check the quality of the mesh in generally. Case-3 geometry was used to simulate the different skewness meshes in this experiment. OF was able to simulate only less than 0.78 maximum skewness meshes. However, AF simulated maximum skewness up to 0.93. This means that AF has more ability to handle low quality mesh than OF.

5.2 Jet mixing comparison between OF and AF

When a fluid mixes with another fluid, velocity shear layers are created between two fluids (Yuan et al., 2004). Ammonia coming out from the small holes can be considered as non-premixed turbulent jet flows. Ammonia mass fraction contours at the first hole is shown in Figure 13 for the both CFD codes. Concentration of ammonia was decreased, when mixing occurred. AF showed comparatively longer shear boundaries. OF shear boundaries were wider than AF boundaries. Figure 14 shows ammonia mass fraction across the jet in a vertical line. The vertical lines are shown in Figure 13. These lines were selected at same distance from the injector pipe. Ammonia mass fraction around the jet was larger in OF while the ammonia mass fraction at the center of the jet was larger in AF. This implies that, higher diffusion was shown in OF and higher convection was shown in AF. This was a reason for the OF showed higher mixing because of higher diffusion effect.

5.3 Vortex street formation comparison

Flow around the cylinder creates turbulent vortexes at Re > 3.5 $\times 10^6$ range (Fluent, 2006). The average Reynolds number was 3.8 $\times 10^6$ in these simulations. Vortex formation comparison around ammonia injecting pipe is shown in Figure 15 (velocity contours). OF showed a higher vortex street formation compared to AF. These high number of vortex streets formation caused the higher mixing level in OF compared to AF. Vortex streets are averaging in steady state simulation but not in transient simulations. OF simulation was in transient mode and AF simulation was in steady state mode. Therefore, transient simulation increased the mixing compared to the steady state simulation.

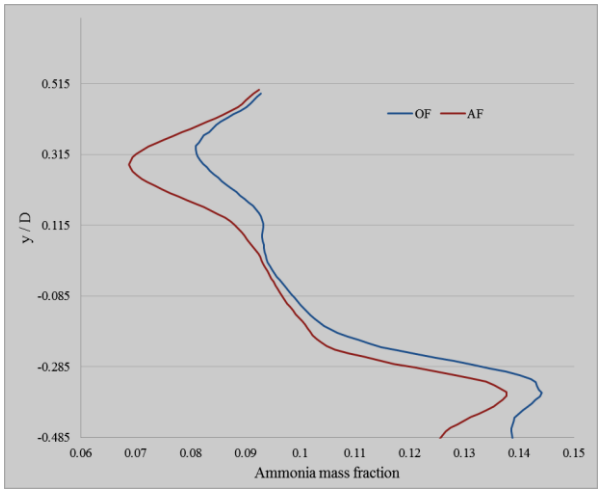

Figure 11. Ammonia mass fraction along the vertical lines at x/D = 4.85(y negative is below the center of plane and vertical lines are shown in Figure 10).

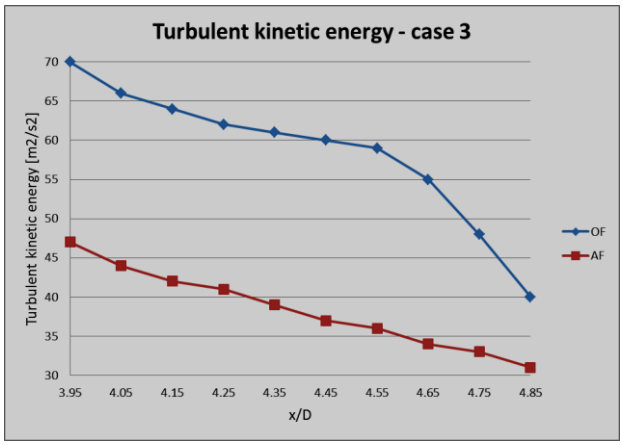

Figure 12. Turbulent kinetic energy comparison – case 3 (Average turbulent kinetic energy in mixing evaluation planes).

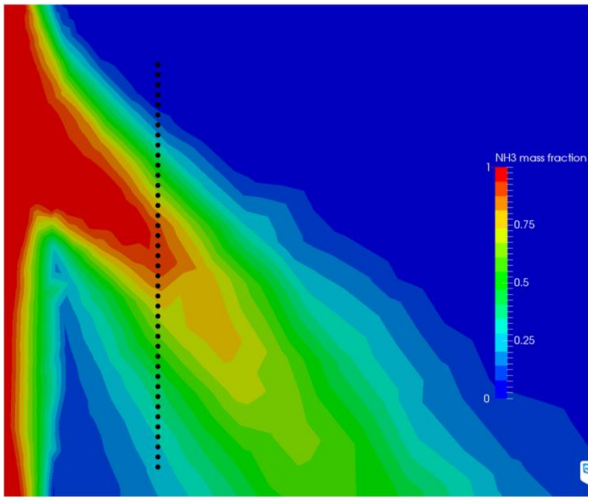

(a)

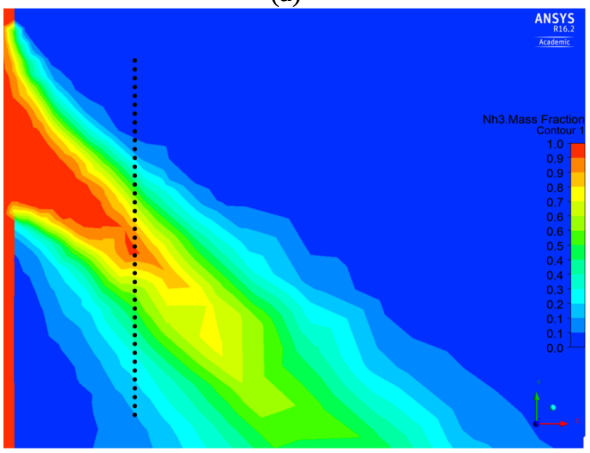

(b)

Figure 13. Jet mixing at first hole in injector; (a) OF, (b) AF.

5.4 Eddy prediction comparison between OF and AF

The standard k-ε model was used by both CFD codes for turbulence prediction. Figure 16 shows large and small eddies in OF and AF. The same locations were

considered for the comparison in both codes. The large eddies were possible to see in between the cylindrical wall and the mixer plates. More large eddies were predicted by AF than OF. However, small eddies were comparatively equally predicted in the both codes.

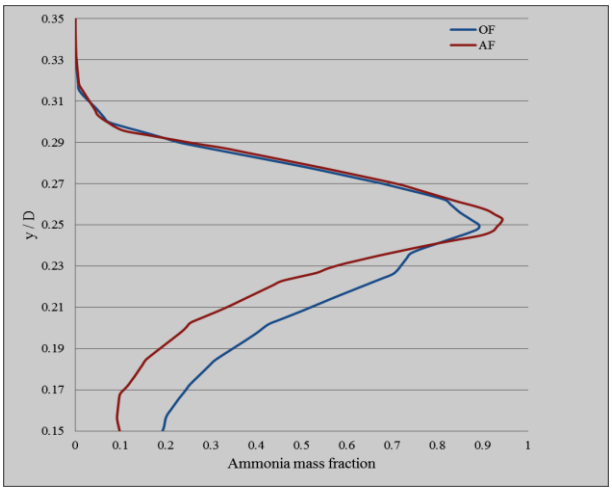

Figure 14. Ammonia mass fraction across a jet (mass fractions were plotted along the vertical lines those lines are shown in Figure 13).

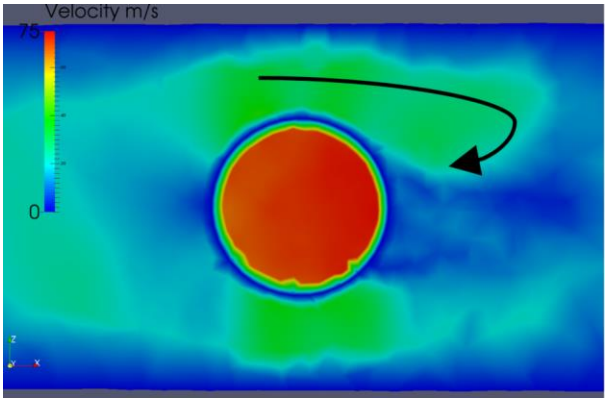

(a)

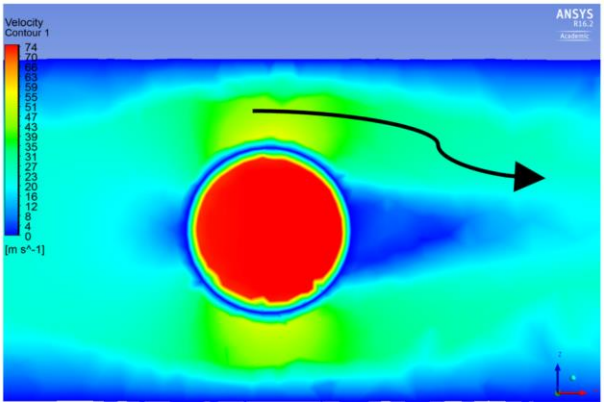

(b)

Figure 15. Vortex street comparison – Velocity contours around ammonia injecting pipe; (a) OF, (b) AF.

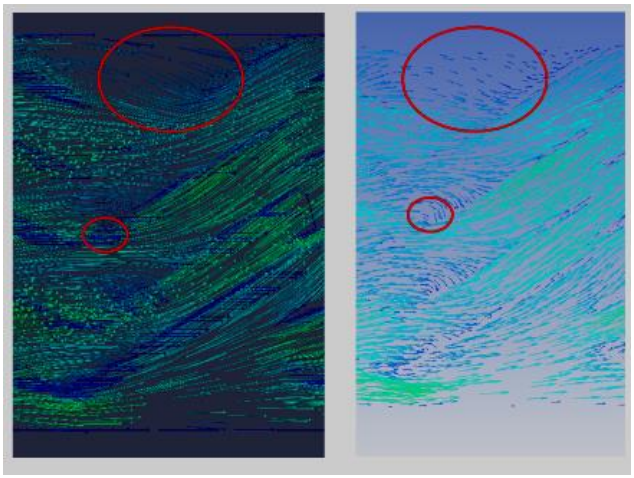

(a) (b)

Figure 16. Large and small eddies (large circles and small circles show large eddies and small eddies respectively); (a) OF, (b) AF.

5.5 Turbulence kinetic energy effect comparison between OF and AF

Energy cascade path starts with main flow energy to large eddies, large eddies energy to small eddies, small eddies energy to smallest eddies and finally to internal energy (Versteeg and Malalasekera, 2007). OF simulation showed higher turbulent kinetic energy than AF in this study. These high turbulent kinetic energies helped to create more vortices in OF according to the energy cascade principle. Because of this, higher mixing was shown in OF compared to AF.

5.6 Summary of OF and AF results comparison

A summary of result comparison is shown in Table 4.

Table 3. Summary of OF and AF results comparison.

Static mixer model	Description
Without static mixer	OF gives higher mixing
With static mixer	Both codes give on average equal mixing

6 Conclusions

Both codes used same constant values for k-ε equation and same initial values. Higher turbulent kinetic energy was predicted from OF compared to AF. As well as higher diffusive properties was shown in OF compared to AF. Those two reasons were mainly involved to predict the higher mixing in OF compared to AF. OF simulation is required higher quality mesh compare to AF. As an example, 0.93 maximum skewness mesh gives a converged result in AF but same mesh gives a diverged result in OF. This implies that finer mesh is

required for OF. Both codes used the ANSYS meshes, which are designed for AF.

Acknowledgment

The authors express their thanks to Luigi Serraiocco, Jakub Bujalski and YARA International ASA for useful technical support.

References

F. Ambrosino and A. Funel. OpenFOAM and Fluent features in CFD simulations on CRESCO High Power Computing system. In *Final Workshop of Grid Projects, PON RICERCA*, 1 – 4, 2006.

M. Balogh, A. Parente, and C. Benocci. RANS simulation of ABL flow over complex terrains applying an Enhanced k-ε model and wall function formulation: Implementation and comparison for fluent and OpenFOAM. *Journal of Wind Engineering and Industrial Aerodynamics*, 104-106: 360–368, 2012. doi:10.1016/j.jweia.2012.02.023

ANSYS Fluent. *Fluent 6.3 Documentation*. Fluent Inc., Lebanon, NH, 2006.

C. J. Greenshields. *Openfoam user guide*. OpenFOAM Found. Ltd, version 3, 2015.

J. B. Kok and S. van der Wal. Mixing in T-junctions. *Applied Mathematical Modelling*, 20: 232–243, 1996. doi:10.1016/0307-904X(95)00151-9

D. A Lysenko, I. S. Ertesvåg, and K. E. Rian. Modeling of turbulent separated flows using OpenFOAM. *Computers & Fluids*, 80: 408–422, 2013. doi:10.1016/j.compfluid.2012.01.015

H. K. Versteeg and W. Malalasekera. *An introduction to computational fluid dynamics: the finite volume method*, 2nd ed. Pearson Education Ltd, 2007.

C. C. L. Yuan, M. Krstić, and T. R. Bewley. Active control of jet mixing. *IEE Proceedings-Control Theory Appl*, 151(6): 763–772, 2004. doi:10.1080/14685248.2014.997244